The Role of Dispersive Forces Determining the Energetics of Adsorption in Ti Zeolites

Matteo Signorile,[a] Alessandro Damin,*[a] Francesca Bonino,[a] Valentina Crocellà,[a] Carlo Lamberti,[a,b,c] and Silvia Bordiga[a,d]

Ti-zeolites are interesting materials because of their key role in partial oxidation reactions, as well as under a fundamental point of view being regarded as single site catalysts. Both experimental and computational approaches have been widely applied to the characterization of their active sites, reaching a level of knowledge unmatchable by most other important catalysts. However, several questions are still open, being a proper energetic simulation of the adsorption process of simple molecules, fitting with the experimental outcomes, still missing. The present work wants to underline the role of dispersive forces in correctly determining the adsorption energies of H_2O and NH_3 in Ti chabazite: first dispersive contributions have been included through an ONIOM scheme, comparing the results from semiempirical Grimme scheme and fully *ab initio* MP2. Being the key contribution of dispersion proved, a fully periodic, Grimme dispersions inclusive approach has been applied, coming to results close to the experimental values. © 2016 Wiley Periodicals, Inc.

Introduction

Ti-zeolites are a class of material covering a relevant niche in the field of heterogeneous catalysis. Characterized by the isomorphous substitution of the framework Si^{4+} with Ti^{4+},[1,2] they mainly find application in partial oxidation reactions in combination with hydrogen peroxide in aqueous solution. Since the largest part of these processes are industrially performed in a liquid, aqueous medium, the interaction of such materials with water is of outmost importance. Further, in most of the cases, ammonia is included in the reaction feeding as stabilizer for the hydrogen peroxide, to prevent its undesired decomposition: being a strong base, NH_3 can easily interact with the Ti sites, positively charged and thus showing a Lewis acid character. The understanding of H_2O/NH_3 interaction with Ti-zeolites is determining in the understanding of their catalytic behavior, as testified by the numerous studies devoted to their characterization.[3–11] Experimentally, the energetic of these interactions has been explored by calorimetric techniques,[3–5] while the coordination sphere and the structure of the Ti sites have been widely explored exploiting vibrational, electronic, and XAS spectroscopies.[11–15] Interesting reviews are available on the characterization of Ti-zeolites.[2,16–20] Some relevant improvements in the interpretation of the outcomes of experimental techniques arise from computational approaches: even with relatively simplified models and low cost computational methods, an accurate description of the vibrational and electronic fingerprints of Ti zeolites has been obtained.[10,15,21] Instead, concerning the energetic of adsorption processes, the results are more diverging from experimental results: according to Bolis and coworkers,[4,5] the measured heat of adsorption for a single NH_3 molecule per Ti site on Titanium Silicalite-1 (TS-1) falls in the range 60–70 kJ mol^{-1} depending on the measurement conditions. Previous computational studies, even if the structural features of the Ti center were properly simulated, were not able to give a right estimation of the interaction energies: cluster calculation on NH_3 mono-adducts showed BSSE corrected binding energies (BE^c) in the 30–40 kJ mol^{-1} range, thereby heavily underestimating the extent of the measured interaction.[7,22,23] It is worth to stress that a cluster approach (also taking in account that the models in the cited works are of relatively small size) does not allow a correct description of the effect of the microporous structure of the zeolite, possibly contributing to the stabilization of the adsorbate. However, also periodic simulation gave rise to very similar results.[6,9,24] A totally analogous situation was observed in the case of water adsorption. To the best of our knowledge, the previous computational studies on Ti-zeolites missed the inclusion/estimation of dispersive interactions, which has been shown to be fundamental in correctly describing the structure of bulk molecular systems (e.g., 3D

structure of proteins and DNA, etc.),[25–27] the adsorption of small molecules (e.g., H_2O, CH_4, small hydrocarbons, etc.) on oxides and zeolites,[28–34] as well as some less obvious properties (e.g., the relative stability of the SiO_2 and TiO_2 polymorphs).[35–37] Accounting for dispersion forces, the size of the considered system plays a relevant role: as recently commented by Wagner and Schreiner: *"For increasingly larger structures, the overall dispersion contribution grows rapidly and can amount to tens of kcalmol^{-1}."*[38] This consideration is of great interest for the adsorption of small molecules in zeolites: the adsorbate, in fact, experiences the dispersive contributions from the whole framework, thus a large effect on the interaction energy is expected. From a quantum mechanical point of view, dispersion forces can be ascribed to the long-range electron correlation: a fully *ab initio* description of these interactions requires the use of correlated methods, such as Møller–Plesset perturbation theory or Coupled Cluster.[39–41] A possible and costless alternative to computationally demanding post Hartree–Fock methods is represented by the empirical estimation of dispersive forces, as introduced by Grimme:[26,42,43] the attractive forces among couples of atoms are evaluated through empirical C^6 coefficients, the reciprocal of the sixth-power of the atom-atom distance and are modulated by an appropriate damping function. In the present work the role of dispersive forces toward the adsorption energetics for ammonia and water in titanium chabazite (here adopted as a test case for Ti-zeolite) is explored: the advantage of such model is the lower size of the unit cell and (if fully exploited) the higher symmetry of the space group in comparison with the complex (but more relevant) TS-1, but showing a very similar environment in the vicinity of the Ti site. It is worth noticing that Ti-CHA was recently synthesized (Si/Ti =246) by the Lillerud group in Oslo[44] and that the spectroscopic responses (IR, UV-Vis, Raman, and Ti K-edge XANES) on water adsorption on Ti sites in Ti-CHA are similar to those observed in TS-1.[11,15] In this work, the results from fully periodic DFT-D are compared with ones obtained through an ONIOM scheme, where dispersive interactions are included exploiting second order Møller-Plesset perturbation theory (MP2). The outcomes of such analysis depict the key role of dispersion forces toward a correct evaluation of the energetic of adsorption processes in Ti-zeolites.

Computational Methods

BE calculation

Binding energies (BE) for the adsorption processes were calculated according to eq. (1)

$$BE = E_a(A) + E_b(B) - E_{ab}(AB) \tag{1}$$

that is, expressing them as the dissociation energy of the *AB* adduct, being *a* and *b* the basis sets for the *A* and *B* monomers, respectively. The BE calculations were performed according to the processes schematized in eqs. (2) and (3), that is, considering two separate dissociations:

$$(AB^1)B^2 \rightarrow AB^1 + B^2 \tag{2}$$

$$AB^1 \rightarrow A + B^1 \tag{3}$$
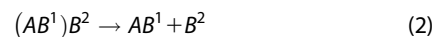
where *A* is TiCHA and B^1 and B^2 are the first and the second ligand respectively. BSSE correction was adopted according to the literature,[45] exploiting the counterpoise method as shown in eq. (4):

$$BE^c = BE - \left[E_a(A^{def}) - E_{ab}(A^{def}) + E_b(B^{def}) - E_{ab}(B^{def}) \right] \tag{4}$$

In such equation, the "def" superscript indicates that the geometry of the monomer after adsorption and relaxation is considered. Substituting eq. (1) in (4) and conveniently rearranging the various terms it is possible to rewrite the latter as:

$$BE^c = \left[E_a(A) - E_a(A^{def}) + E_b(B) - E_b(B^{def}) \right] + \left[E_{ab}(A^{def}) + E_{ab}(B^{def}) - E_{ab}(AB^{def}) \right] \tag{5}$$

The second term is now split in two distinct contributions: the former takes in account the purely deformational contribution to the BEs, that is, the deformation energy (DE); the latter represents the BSSE corrected BE for the adduct calculated starting from the already deformed monomers, indeed it takes in account the energetic contributions to the BE^c due to the monomers interaction only and it will be labeled as BE^{defc}. On the basis of such consideration, eq. (5) can be further rewritten as:

$$BE^c = DE + BE^{defc} \tag{6}$$

being

$$DE = E_a(A) - E_a(A^{def}) + E_b(B) - E_b(B^{def}) \tag{7}$$

$$BE^{defc} = E_{ab}(A^{def}) + E_{ab}(B^{def}) - E_{ab}(AB) \tag{8}$$

All these considerations are valid (and thus they were exploited) for both periodic and ONIOM calculations.

Periodic computations

The periodic model of TiCHA was built up starting from the experimental geometry of purely siliceous chabazite:[46] a supercell [whose lattice parameters a', b', c' were derived from single cell ones a, b, c according to eq. (9)] was obtained.

$$a' = -a + b + c$$
$$b' = a - b + c \tag{9}$$
$$c' = a + b - c$$

Such supercell contains 144 atoms and 48 equivalent Si sites. Consequently, a single silicon atom was substituted by a titanium one giving rise to a TiCHA model with Si/Ti ratio of 47 (corresponding to ∼2.75 wt% of framework TiO_2, where typical TS-1 samples contain about 2 wt% TiO_2): the introduction of titanium causes the space group of the system to change

from Rm to P1, that is, the successive calculations were performed without taking advantage of the symmetry. The model was relaxed and exploited as starting point for the following adsorption simulation. Ammonia and water adsorption on the Ti site were studied. For both molecules, single and double coverage were considered: in the case of the adsorption of the second molecule, the relaxed geometry of the single adduct was used as starting point for the calculation. The periodic calculations were performed with the CRYSTAL14 code[47]: the B3LYP functional, combining the B3[48] hybrid exchange functional with the LYP[49] correlation functional, was exploited. A double ζ quality basis set was employed in the description of the periodic framework: 86-411G(d31) for Ti,[50] 88-31G(d1) for Si and 8-411G(d1) for O.[51] These basis sets are explicitly reported in Tables S1 of the Supporting Information. In the description of adsorbates, Ahlrichs TZV2P and TZV basis sets were exploited in the description of O/N and H respectively.[52] Thresholds for the mono- and bi-electronic integral (TOLINTEG) were set to {777714}. The shrinking factor parameters (SHRINK), determining the k-points sampling in the reciprocal space, were set to {2 2}. The maximum order of shell multipoles in the long-range zone for the electron-electron Coulomb interaction (POLEORDR keyword) was chosen to be 6. The defaults values for all the unreported computational parameters were used.[53] Dispersive forces were included in the calculation when required as implemented in the CRYSTAL code, that is, accordingly to the Grimme two bodies (GD2) scheme.[53]

ONIOM computations

The ONIOM2 (hereafter simply labeled as ONIOM) scheme as proposed by Morokuma et al. was applied in this work.[54] In this approach, the system is partitioned in two distinct layers: an inner part, containing the site of interest for the simulation (the so called model region), and the whole system (labeled as real model). For obvious reasons, the model region is treated with a higher level of theory (being so defined as High Model, HM), whereas for the real layer a less costly method (Low Real, LR) can be used. The ONIOM BE is then computed as reported in eq. (10):

$$BE(ONIOM) = BE(LR) - BE(LM) + BE(HM) \quad (10)$$

To properly compute the ONIOM energy, the contribution from the model region calculated at the low level method (Low Model, LM) is included in eq. (10). The presented ONIOM computations consist of single point energy calculations, adopting as LR the periodic TiCHA/TiCHA + NH$_3$ structures obtained from periodic calculations at the B3LYP level (see "Periodic computations" section for further details). Clusters of increasing size were considered as model region, ranging from 9 up to 55 real framework atoms (i.e., involving a fraction of the total atoms χ in the $0.06 < \chi < 0.38$ range). Their structure, in the form of NH$_3$ adducts, are schematized in Figure 1.

The dangling bonds on Si centers were saturated by hydrogen atoms, placed at a fixed distance of 1.45 Å along pristine
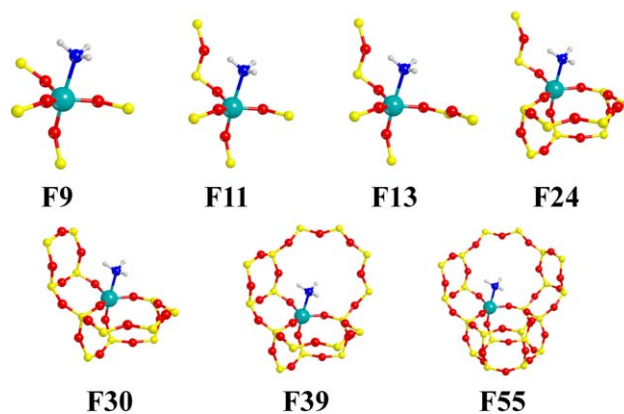

Figure 1. Ball and stick representation of the clusters used in the ONIOM calculations. [Color figure can be viewed at wileyonlinelibrary.com]

Si—O bonds. HM calculations on the model clusters were performed adopting B3LYP, B3LYP-D and MP2 methods. The B3LYP, B3LYP-D calculations on all the clusters, as well as the MP2 ones on clusters from F9 to F24, were performed exploiting the Gaussian09 code.[55] For the three bulkier clusters (F30, F39, F55), the MP2 calculations were performed with NWChem to exploit the massive parallelization offered by the code.[56] In both cases, the MP2 calculations were limited to the valence electrons, freezing instead the core ones. A Dunning aug-cc-pVQZ basis set was chosen for anions (O and N), an Ahlrichs TZVP for cations (Ti and Si) and a Pople 6-311++G(2p,2d) for H atoms. All the G09/NWChem default computational parameters were used in the calculation. LM calculations on the model region were performed exploiting the CRYSTAL14 code, at the B3LYP level and with the same parameters used for the periodic calculations.

Results and Discussion

Periodic construction of the starting TiCHA(+NH$_3$) model

As starting model for the following calculations, TiCHA and TiCHA + NH$_3$ periodic models were optimized without including dispersive forces. The optimized cell volume and the distances among the Ti center and its O/N first neighbors are reported in Table 1.

The full set of relaxed cell parameters is given in Supporting Information Table S2. The introduction of the Ti atom in the siliceous framework of CHA leads to a slight expansion of the cell as demonstrated by the increase of the cell parameters and, consequently, of the cell volume. This expansion is due to the average Ti—O distance falling in the 1.79–1.81 Å range,[4,5,13,14,57] thus much larger than the typical average Si—O distance in zeolites of about 1.60 Å.[46,58] Conversely, the cell angles are only slightly modified. The extent of the expansion, about 0.6%, is closely matching the experimental evidences obtained on TS-1, where diffraction experiments showed an increase of the cell volume of 0.8% at similar Ti contents.[59] By comparison, the geometry relaxation performed on a TiCHA model based on a single CHA cell (Si/Ti = 11)[9] leaded to an unrealistic cell volume expansion of about 3% (see Table S3 of

Table 1. B3LYP optimized cell volumes, Ti—O and Ti—N bond lengths for the CHA, TiCHA, and TiCHA + NH_3 periodic models.

Model	Cell volume (Å^3)	Ti—O_{ap} (Å)	Ti—O_{eq1} (Å)	Ti—O_{eq2} (Å)	Ti—O_{eq3} (Å)	<Ti—O> (Å)	Ti—N (Å)
CHA	3243	–	–	–	–	–	–
Ti-CHA	3263	1.803	1.799	1.794	1.809	1.801	–
Ti-CHA+NH_3	3259	1.844	1.821	1.809	1.838	1.828	2.359

the Supporting Information). Introducing the NH_3 adsorbate a negligible reduction of the cell size is observed, whereas in the case of the single cell model a reduction of −0.4% was computed. The reported data confirmed the good choice of a supercell model, as its realistic Ti loading allows to properly describe the system. Looking closer at the Ti coordination sphere, on ammonia adsorption the observed deformation effects are more evident. The unperturbed Ti site exhibits an almost perfectly tetrahedral local symmetry and an average Ti—O distance in good agreement with the experimental distance of 1.79 Å obtained on dehydrated TS-1 by EXAFS.[4,5,13,14,57] After the NH_3 adsorption, the local geometry of the Ti site is significantly altered: all the Ti—O distances are enlarged (as experimentally observed by EXAFS) and the local T_d symmetry is broken. In particular, the distance between Ti and the O in apical position with respect to the NH_3 is the most affected, whereas the equatorial oxygen atoms react in a heterogeneous way to the adsorption. Considering the average Ti—O distance in the NH_3 adduct, this is slightly underestimated in comparison with the experimental values (1.88 Å for EXAFS, measurements with 2 adsorbed NH_3 molecules per Ti atom), however the correct trend (i.e., expansion) is observed as already commented.[5,16] The seven clusters used in the ONIOM calculations (which structures are depicted in Fig. 1) were extracted from these periodic models. The calculated BE^c are reported in Table 2 and graphically outlined in Figure 2.

Concerning the low model, the BSSE corrected BEs rapidly converge to the value calculated for the full, low real periodic model: the larger increases of the BE^c(LM) observed on the first cluster enlargements can be ascribed to a proper inclusion of the major electrostatic contributions, whereas this growth is reduced as atoms farer from the Ti site are added to the model region. Unexpectedly, the last two clusters exhibit again a large BE^c(LM) in comparison to the previous ones; furthermore, a small reduction in the BE^c(LM) is observed moving from cluster F39 to the much bigger F55. Despite this oscillating behavior (no more than 6 kJ mol^{-1}), possibly due to bad compensation among the three layers, a reasonable overall convergence is achieved. This interpretation is confirmed by looking at the energetic of the B3LYP//B3LYP$_{CRY}$ high models: exploiting the higher precision proper of a molecular calculation the BE^c(HM) shows a smoother, monotonic trend also in the bigger clusters. Also in this case, a fast convergence to the BE^c(LR) value is observed. As a consequence of the larger value of BE^c(LM) compared to BE^c(LR), the ONIOM BEs for the bigger clusters are smaller than the respective for the HM; however it is worth to underline that also in these cases the energy difference between BE^c(HM) and BE^c(ONIOM) is below 3 kJ mol^{-1}, a significantly small value thus allowing a proper comparison with the experimental values. All the results achieved without including dispersive forces are in good agreement with the previous computational literature,[7,9] so largely underestimating the TiCHA-NH_3 interaction energy. The situation totally changes as dispersions are considered, both empirically (B3LYP-D//B3LYP$_{CRY}$) or *ab initio* (MP2//B3LYP$_{CRY}$): also for the smaller clusters, the BE is significantly increased, rapidly converging to the B3LYP-D$_{CRY}$//B3LYP$_{CRY}$ BE^c(LR) reference value. The difference between the BE^c(HM) computed at B3LYP-D//B3LYP$_{CRY}$ and at B3LYP//B3LYP$_{CRY}$ represents the purely dispersive contribution to the BE: the value of 23.4 kJ mol^{-1} obtained for the smaller cluster (F9) reaches the 34.3 kJ mol^{-1} for the bigger one (F55), with an increase of

Table 2. HM and ONIOM BSSE corrected Binding Energies (BE^c) for the seven model cluster at different computational levels.

Model	F9	F11	F13	F24	F30	F39	F55	LR
χ	0.06	0.08	0.09	0.17	0.21	0.27	0.38	1.00
B3LYP$_{CRY}$								
BE^c (LR)	–	–	–	–	–	–	–	29.6
BE^c (LM)	11.1	15.7	21.3	25.2	26.4	33.1	32.1	–
B3LYP-D$_{CRY}$//B3LYP$_{CRY}$								
BE^c (LR)	–	–	–	–	–	–	–	67.1
B3LYP//B3LYP$_{CRY}$								
BE^c (HM)	12.0	15.7	20.2	24.3	24.7	30.3	30.4	–
BE^c (ONIOM)	30.5	29.6	28.5	28.7	27.9	26.8	27.9	–
B3LYP-D//B3LYP$_{CRY}$								
BE^c (HM)	35.4	41.9	48.0	53.2	55.6	63.7	64.7	–
BE^c (ONIOM)	53.9	55.8	56.4	57.5	58.9	60.2	62.1	–
MP2//B3LYP$_{CRY}$								
BE^c (HM)	35.3	40.9	46.9	52.3	55.0	63.2	63.8	–
BE^c (ONIOM)	53.8	54.9	55.2	56.7	58.2	59.7	61.2	–

All the value are reported in kJ mol^{-1}. χ represent the fraction of unit cell atoms included in the cluster. Reported values are plotted in Figure 2 as a function of the fraction of unit cell atoms included in the cluster χ.
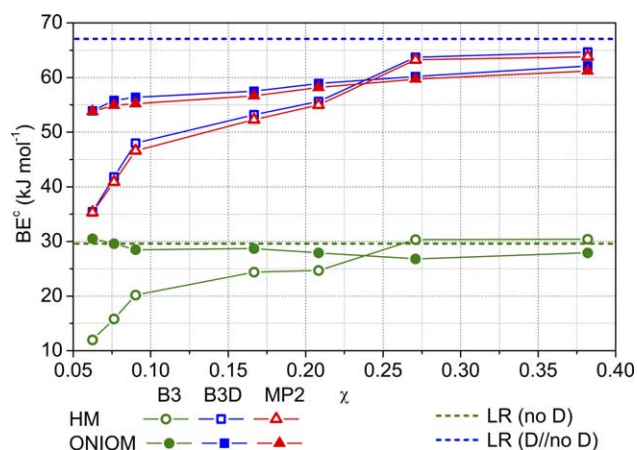
Figure 2. High Model (HM) and ONIOM BE^c versus the fraction of real atoms included in the model region with respect to the low real model (χ), computed at the B3LYP (B3), B3LYP-D (B3D), and MP2 levels. The BE^c computed for the Low Real (LR) periodic model without including dispersions (no D) and adding them *a posteriori* (D//no D) are reported as references. See also Table 2. [Color figure can be viewed at wileyonlinelibrary.com]

10.9 kJ mol^{-1}. By comparison, the dispersive contribution calculated on the BE^c(LR) is 37.5 kJ mol^{-1}: such result demonstrates that the F55 fragment is sufficiently big to take in account the 91% of the total dispersive contribution, being so an effective model in describing the NH_3 adsorption on TiCHA even with a cluster approach. A quite similar result is achieved by including dispersive forces *ab initio* through the correlated MP2 method: the computed BEs are of the same magnitude of B3LYP-D/B3LYP$_{CRY}$, being in average 0.5 kJ mol^{-1} lower. To verify the accuracy of the calculation, a complete basis set extrapolation on the BE^c(HM) for the F9 model was performed: comparing the values obtained with the aug-cc-pVQZ basis with ones extrapolated at CBS these are really similar, testifying the goodness of the adopted approach (see Supporting Information Fig. S1 and Table S4 for details). On this model, also CCSD and CCSD(T) calculation and CBS extrapolation were performed: the former leaded to results in line with the MP2 ones, while the latter showed an energy gain of about 3 kJ mol^{-1}. However, MP2 can be regarded as a reasonable benchmark method in this study, also considering the almost unaffordable cost of coupled cluster calculations. To better characterize the contributions to the BE^c, the DE and the BEs

for the already deformed monomers (BE^{defc}) were computed as reported in Table 3.

It is possible to observe that the DE is pretty similar among the different methods, as well as considering the different clusters sizes. Conversely the BE^{defc} is approximately 40% larger when dispersions are included (both empirically or *ab initio*) and it increases as the cluster size increases. This result suggest the importance of dispersive forces in correctly simulating the TiCHA-NH_3 interaction: the bonding and nonbonding electrostatic contributions determine about the 60% of the final BE and, since the energy contribution from deformation is in first approximation constant, the missing fraction of the BE^c is univocally ascribable to dispersive forces.

Fully periodic approach

Since the key role of dispersive forces has been demonstrated, a fully periodic, dispersions inclusive (through the Grimme GD2 scheme) approach to the complexation of TiCHA with ammonia and water was exploited. The dispersive contributions were directly included in the geometry relaxation. The obtained relaxed structures are sketched in Figure 3. The optimized cell volumes for the H_2O and NH_3 mono- and bi-adducts with TiCHA are shown in Table 4 together with the Ti—O and Ti—Ligand distances.

The detailed relaxed cell parameters are given in Supporting Information Table S5. The data for the bare CHA and TiCHA are reported as well. Even if the dispersive interactions are included in the geometry relaxation, the expansion due to the Ti insertion in the CHA framework gives a result closer to the experimental one, reaching in this case the 0.8%. Furthermore, the reliability of the supercell model allows to perform the adsorption simulations with negligible geometrical deformation of the zeolitic framework. Only in the case of double ammonia adsorption the cell volume is significantly reduced, being similar to the one of the bare CHA. Concerning the local structure of the Ti center, the average Ti—O distance on adsorption is increased: in the case of NH_3 the introduction of a second adsorbed molecule brings closer to the expected experimental value of 1.88 Å.[4,5] In the case of water conversely the average Ti—O value for a single adsorption is matching experimental one (1.82 Å), whereas it is slightly overestimated for the second adsorption.[5,16] However the general

Table 3. Deformation energies (DE) and the BE for the already deformed monomers (BE^{defc}) for the seven model cluster at different computational levels.

| Model | χ | B3LYP//B3LYP$_{CRY}$ | | B3LYP-D//B3LYP$_{CRY}$ | | MP2//B3LYP$_{CRY}$ | |
		DE	BE^{defc}	DE	BE^{defc}	DE	BE^{defc}
F9	0.06	−44.6	56.6	−43.7	79.1	−42.7	78.0
F11	0.08	−42.6	58.2	−41.6	83.4	−40.6	81.5
F13	0.09	−40.5	60.7	−39.0	87.0	−38.2	85.0
F24	0.17	−40.7	65.0	−39.2	92.4	−37.8	90.1
F30	0.21	−41.5	66.2	−39.8	95.4	−38.1	93.0
F39	0.27	−40.5	70.8	−39.0	102.7	−36.6	99.8
F55	0.38	−40.9	71.3	−39.1	103.7	−36.9	100.6

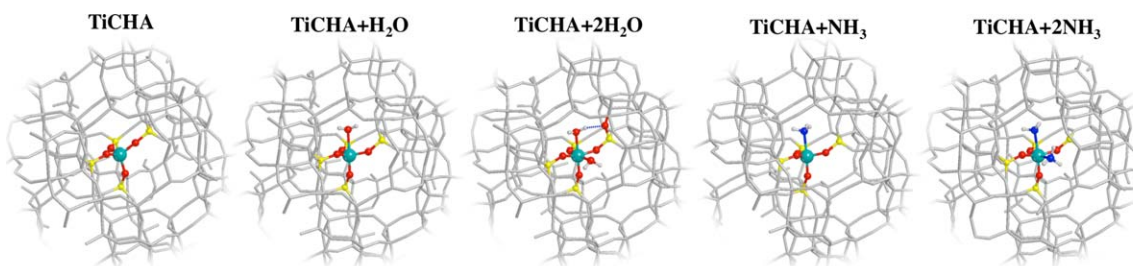All the value are reported in kJ mol^{-1}.

Figure 3. Graphical representation of the periodic models after relaxation. [Color figure can be viewed at wileyonlinelibrary.com]

Table 4. B3LYP-D optimized cell volumes, Ti—O and Ti—L (where L is the N/O atom of the adsorbate) bond lengths for the CHA, TiCHA, and TiCHA + H_2O/NH_3 mono- and bi-adducts periodic models.

Model	Cell volume (Å³)	Ti—O_{ap} (Å)	Ti—O_{eq1} (Å)	Ti—O_{eq2} (Å)	Ti—O_{eq3} (Å)	<Ti—O> (Å)	Ti—L^1 (Å)	Ti—L^2 (Å)
CHA	3180	–	–	–	–	–	–	–
Ti-CHA	3204	1.809	1.781	1.802	1.806	1.799	–	–
Ti-CHA + H_2O^1	3208	1.832	1.808	1.818	1.824	1.820	2.379	–
+ H_2O^2	3201	1.882	1.831	1.840	1.848	1.850	2.263	2.330
Ti-CHA + NH_3^1	3202	1.840	1.802	1.834	1.839	1.829	2.328	–
+ NH_3^2	3183	1.868	1.853	1.855	1.868	1.861	2.343	2.307

description of the Ti-site local environment is quite reliable and phenomenologically sound. Considering the Ti—L distances, fairly different behavior are observed for water and ammonia: in the case of H_2O, when the second molecule is adsorbed the Ti—L^1 distance is reduced, becoming smaller than the Ti—L^2 one; conversely for NH_3 a slight increase of Ti—L^1 is observed on the second adsorption, whereas the Ti—L^2 is shorter than the previous. The shortening of the Ti—L^1 distance for water is explained by the formation of a hydrogen bond among the H_2O molecule and an oxygen framework atom (a third neighbor of Ti) allowed by the framework deformation induced by the second adsorption. Since the water oxygen is now more polarized, it becomes able to interact stronger with the Ti center, that is, a shorter Ti—OH_2 distance is observed. In the case of ammonia, the second adsorption induces a sudden change in the system, as already inferred after the unexpected volume reduction. The addition of a second NH_3 molecule is probably able to significantly detach the Ti from the framework, as the considerable increase in the average Ti—O distances testifies. The framework response to this "detachment" is represented by a partial recovery of its original, siliceous structure as the volume contraction to values proper of CHA model suggests. Regarding

the energetics of the adsorption processes, the BE^c values reported in Table 5 are in good agreement with the experimental data.

Referring to the data of Bolis and coworkers on NH_3 adsorption,[4,5] a heat of adsorption of 66 kJ mol⁻¹ is expected for a single adsorption whereas a slightly lower one (55 kJ mol⁻¹) is ascribed to the second one: the computed BEs (69.6 kJ mol⁻¹ for single and 52.2 kJ mol⁻¹ for double adsorption respectively) are for the first time approaching the experimental values. Similarly, the literature value expected for water adsorption (of about 50 kJ mol⁻¹) is correctly reproduced.[3] It is important to note that a proper comparison should be performed with calculated enthalpies, thus requiring a full frequency calculation to estimate the zero point energy, the thermal energy and the pV contributions: being this kind of calculation really costly on the chosen periodic system, it has not been considered in the present work. However, at least in an approximate ground, the agreement with experimental data is really promising and it demonstrates the reliability of the TiCHA model in the simulation of adsorption on Ti zeolites. Considering the DE and BE^{defc}, as already commented in relation to geometrical parameters, the trends observed for water and ammonia adsorption are substantially different. For the H_2O adsorption a reduction of both DE and BE^{defc} on the introduction of the second molecule is computed, consistently with a pure adsorption process: the first molecule causes the deformation of the framework and strongly interacts with the Ti, whereas the following insertion of the second one requires a lower DE but also give rise to a weaker interaction. Consequently, the BE^c for the second adsorption is lower than the first as expected. Conversely, in the case of NH_3, the second adsorption requires a much larger DE to move the Ti atom in its new "quasi-extraframework" position, being the whole zeolite framework seriously involved in a partial reconversion toward

Table 5. B3LYP-D BSSE corrected binding energies (BE^c), DE, and the BE for the already deformed monomers (BE^{defc}) for the TiCHA and TiCHA + H_2O/NH_3 mono- and bi-adducts periodic models.

Model	BE^c	DE	BE^{defc}
Ti-CHA + H_2O^1	50.8	−35.8	86.7
+ H_2O^2	45.7	−32.2	78.0
Ti-CHA + NH_3^1	69.6	−48.3	118.0
+ NH_3^2	52.2	−62.4	114.6
All the value are reported in kJ mol⁻¹.			

a pure-siliceous like structure. However the new ligand is fundamental in stabilizing the new local structure of the Ti, as testified by the slight reduction of the BE^{defc} with respect to the first adsorption process.

Conclusions

The present work demonstrated the importance of dispersive forces in the correct evaluation of adsorption energetics of water and ammonia on a model Ti-zeolite (TiCHA). Independently from the method chosen for their evaluation (empirical Grimme scheme or *ab initio* MP2), the inclusion of dispersions in the ONIOM approach give rise to an increase (about 50%) of the final BE, so having a comparable weight compared to the purely electrostatic and charge transfer contributions. Strong of this result, water and ammonia adsorptions with single and double coverages were performed with a fully periodic approach and including empirically dispersive forces. The outcomes interestingly underlined the different behavior of the two molecules, with the water being simply adsorbed, whereas a reactivity toward Ti is inferred for ammonia (at least at the highest coverage). These findings are really relevant since they can represent the starting point for a de-titanation processes possibly occurring at the reaction condition, arousing a change in the Ti sites speciation and thus determining an irreversible modification of the overall catalytic activity of the Ti-zeolite. It is finally worth comparing our calculation data with the recent experimental work of Gallo et al.,[11] who used valence to core X-ray emission spectroscopy (vtc-XES)[60–62] to investigate TS-1 before and after interaction with H_2O and NH_3. In that work authors found that, for both adsorbates, the experimental vtc-XES maps were better reproduced by the theoretical maps computed on the basis of a cluster containing only one ligand molecule rather than two. This finding is in apparent contradiction with the computational results reported here, where the addition of a second ligand has BE^c values comparable to that of the first absorbed molecule (see Table 5), thereby making the insertion of a second ligand (H_2O or NH_3) energetically favored. The disagreement between these two studies may be cured by considering the three aspects. (i) The high photon flux emitted by the two ondulators of the ID26 beamline of the ESRF may cause a photon-induced desorption of the second ligand. (ii) The theoretical vtc-XES maps computed by Gallo et al.[11] were obtained on a large cluster, but without taking into account the effect of the dispersive interactions as done here. (iii) While the Ti-CHA framework exhibits only one crystallographic independent T sites, TS-1 (MFI topology) has 12. This means that all Ti atoms inserted in the CHA framework will have the same local environment, having room to host up to two ligands. Instead, some of the T sites of the MFI framework, found to be favorable for Ti insertion by neutron diffraction data,[63] are more sterically hindered by surroundings because of the different channel topology. This is the case of sites T7 and T11, whereas T6 site, sitting at the channels intersection of the MFI structure, could coordinate up to two ligands (H_2O or NH_3).

How to cite this article: M. Signorile, A. Damin, F. Bonino, V. Crocellà, C. Lamberti, S. Bordiga. *J. Comput. Chem.* **2016**, DOI: 10.1002/jcc.24509

Additional Supporting Information may be found in the online version of this article.

[1] B. Notari, G. Perego, M. Taramasso, *Preparation of Porous Crystalline Synthetic Material Comprised of Silicon and Titanium Oxides* **1983**, US4410501 A.

[2] B. Notari, In *Advances in Catalysis;* D. D. Eley, W. O. Haag, B. Gates ,Eds.; Elsevier Academic Press Inc: San Diego, **1996**; pp. 253–334.

[3] T. Blasco, M. Camblor, A. Corma, P. Esteve, J. M. Guil, A. Martı, S. Valencia, A. Martinez, J. Perdigon-Melon, *J. Phys. Chem. B* **1998**, *102*, 75.

[4] V. Bolis, S. Bordiga, C. Lamberti, A. Zecchina, A. Carati, F. Rivetti, G. Spanò, G. Petrini, *Langmuir* **1999**, *15*, 5753.

[5] V. Bolis, S. Bordiga, C. Lamberti, A. Zecchina, A. Carati, F. Rivetti, G. Petrini, G. Spanò, *Microporous Mesoporous Mater.* **1999**, *30*, 67.

[6] C. M. Zicovich-Wilson, R. Dovesi, A. Corma, *J. Phys. Chem. B* **1999**, *103*, 988.

[7] A. Damin, S. Bordiga, A. Zecchina, C. Lamberti, *J. Chem. Phys.* **2002**, *117*, 226.

[8] S. Bordiga, A. Damin, F. Bonino, G. Ricchiardi, A. Zecchina, R. Tagliapietra, C. Lamberti, *Phys. Chem. Chem. Phys.* **2003**, *5*, 4390.

[9] A. Damin, S. Bordiga, A. Zecchina, K. Doll, C. Lamberti, *J. Chem. Phys.* **2003**, *118*, 10183.

[10] E. Fois, A. Gamba, G. Tabacchi, *ChemPhysChem* **2008**, *9*, 538.

[11] E. Gallo, F. Bonino, J. C. Swarbrick, T. Petrenko, A. Piovano, S. Bordiga, D. Gianolio, E. Groppo, F. Neese, C. Lamberti, P. Glatzel, *ChemPhysChem* **2013**, *14*, 79.

[12] D. Scarano, a. Zecchina, S. Bordiga, F. Geobaldo, G. Spoto, G. Petrini, G. Leofanti, M. Padovan, G. Tozzola, *J. Chem. Soc. Faraday Trans.* **1993**, *89*, 4123.

[13] S. Bordiga, F. Boscherini, S. Coluccia, F. Genonic, C. Lamberti, G. Leofanti, L. Marchese, G. Petrini, G. Vlaic, A. Zecchina, *Catal. Lett.* **1994**, *26*, 195.

[14] S. Bordiga, S. Coluccia, C. Lamberti, L. Marchese, A. Zecchina, F. Boscherini, F. Buffa, F. Genoni, G. Leofanti, *J. Phys. Chem.* **1994**, *98*, 4125.

[15] G. Ricchiardi, A. Damin, S. Bordiga, C. Lamberti, G. Spano, F. Rivetti, A. Zecchina, G. Spanò, F. Rivetti, A. Zecchina, *J. Am. Chem. Soc.* **2001**, *123*, 11409.

[16] S. Bordiga, F. Bonino, A. Damin, C. Lamberti, *Phys. Chem. Chem. Phys.* **2007**, *9*, 4854.

[17] P. Ratnasamy, D. Srinivas, H. Knözinger, *Adv. Catal.* **2004**, *48*, 1.

[18] S. Bordiga, E. Groppo, G. Agostini, J. A. van Bokhoven, C. Lamberti, *Chem. Rev.* **2013**, *113*, 1736.

[19] L. Nemeth, S. R. Bare, *Adv. Catal.* **2014**, *57*, 1.

[20] J. A. van Bokhoven, C. Lamberti, *Coord. Chem. Rev.* **2014**, *277*, 275.

[21] S. Bordiga, A. Damin, F. Bonino, A. Zecchina, G. Spanò, F. Rivetti, V. Bolis, C. Prestipino, C. Lamberti, *J. Phys. Chem. B* **2002**, *106*, 9892.

[22] P. E. Sinclair, G. Sankar, C. R. A. Catlow, J. M. Thomas, T. Maschmeyer, *J. Phys. Chem. B* **1997**, *101*, 4232.

[23] H. Munakata, Y. Oumi, A. Miyamoto, *J. Phys. Chem. B* **2001**, *105*, 3493.

[24] G. Ricchiardi, A. de Man, J. Sauer, *Phys. Chem. Chem. Phys.* **2000**, *2*, 2195.

[25] P. Ugliengo, A. Damin, *Chem. Phys. Lett.* **2002**, *366*, 683.

[26] S. Grimme, *J. Comput. Chem.* **2004**, *25*, 1463.

[27] J. Antony, S. Grimme, *Phys. Chem. Chem. Phys.* **2006**, *8*, 5287.

[28] T. Kerber, M. Sierka, J. Sauer, *J. Comput. Chem.* **2008**, *29*, 2088.

[29] S. Tosoni, J. Sauer, *Phys. Chem. Chem. Phys.* **2010**, *12*, 14330.

[30] R. Włodarczyk, M. Sierka, K. Kwapień, J. Sauer, E. Carrasco, A. Aumer, J. F. Gomes, M. Sterrer, H. J. Freund, *J. Phys. Chem. C* **2011**, *115*, 6764.

[31] A. Rimola, D. Costa, M. Sodupe, J. F. Lambert, P. Ugliengo, *Chem. Rev.* **2013**, *113*, 4216.

[32] N. Kumar, P. R. C. Kent, D. J. Wesolowski, J. D. Kubicki, *J. Phys. Chem. C* **2013**, *117*, 23638.

[33] G. Piccini, M. Alessio, J. Sauer, Y. Zhi, Y. Liu, R. Kolvenbach, A. Jentys, J. A. Lercher, *J. Phys. Chem. C* **2015**, *119*, 6128.

[34] M. Delle Piane, M. Corno, R. Orlando, R. Dovesi, P. Ugliengo, *Chem. Sci.* **2016**, *7*, 1496.

[35] J. Moellmann, S. Ehrlich, R. Tonner, S. Grimme, *J. Phys. Condens. Matter.* **2012**, *24*, 424206.

[36] H. Hay, G. Ferlat, M. Casula, A. P. Seitsonen, F. Mauri, *Phys. Rev. B Condens. Matter Mater. Phys.* **2015**, *92*, 144111.

[37] E. I. Román-Román, C. M. Zicovich-Wilson, *Chem. Phys. Lett.* **2015**, *619*, 109.

[38] J. P. Wagner, P. R. Schreiner, *Angew. Chem. Int. Ed.* **2015**, *54*, 12274.

[39] S. Kristyán, P. Pulay, *Chem. Phys. Lett.* **1994**, *229*, 175.

[40] P. Hobza, J. Sponer, T. Reschel, *J. Comput. Chem.* **1995**, *16*, 1315.

[41] M. J. Allen, D. J. Tozer, *J. Chem. Phys.* **2002**, *117*, 11113.

[42] S. Grimme, *J. Comput. Chem.* **2006**, *27*, 1787.

[43] S. Grimme, J. Antony, S. Ehrlich, H. Krieg, *J. Chem. Phys.* **2010**, *132*, 154104 1.

[44] E. A. Eilertsen, S. Bordiga, C. Lamberti, A. Damin, F. Bonino, B. Arstad, S. Svelle, U. Olsbye, K. P. Lillerud, *ChemCatChem* **2011**, *3*, 1869.

[45] G. Lendvay, I. Mayer, *Chem. Phys. Lett.* **1998**, *297*, 365.

[46] M.-J. Díaz-Cabañas, P. A. Barrett, *Chem. Commun.* **1998**, *17* 1881.

[47] R. Dovesi, R. Orlando, A. Erba, C. M. Zicovich-Wilson, B. Civalleri, S. Casassa, L. Maschio, M. Ferrabone, M. De La Pierre, P. D'Arco, Y. Noël, M. Causá, M. Rérat, B. Kirtman, *Int. J. Quantum Chem.* **2014**, *114*, 1287.

[48] A. D. Becke, *J. Chem. Phys.* **1993**, *98*, 1372.

[49] C. Lee, W. Yang, R. G. Parr, *Phys. Rev. B* **1988**, *37*, 785.

[50] Crystal.unito.it. **2016**. Available at: http://www.crystal.unito.it/Basis_Sets/titanium.html#Ti_86- 411%28d31%29G_darco_unpub.

[51] R. Nada, J. B. Nicholas, M. I. McCarthy, A. C. Hess, *Int. J. Quantum Chem.* **1996**, *60*, 809.

[52] A. Schäfer, C. Huber, R. Ahlrichs, *J. Chem. Phys.* **1994**, *100*, 5829.

[53] R. Dovesi, V. R. Saunders, C. Roetti, R. Orlando, C. M. Zicovich-Wilson, F. Pascale, B. Civalleri, K. Doll, N. M. Harrison, I. J. Bush, Ph. D'Arco, M. Llunel, M. Causá, Y. Nöel8, CRYSTAL14 User's Manual. **2016** Available at: http://www.crystal.unito.it/Manuals/crystal14.pdf **2014**.

[54] S. Dapprich, I. Komáromi, K. S. Byun, K. Morokuma, M. J. Frisch, *J. Mol. Struct. Theochem* **1999**, *461–462*, 1.

[55] M. J. Frisch, G. W. Trucks, H. B. Schlegel, G. E. Scuseria, M. A. Robb, J. R. Cheeseman, G. Scalmani, V. Barone, B. Mennucci, G. A. Petersson, M. J. Frisch, G. W. Trucks, H. B. Schlegel, G. E. Scuseria, M. A. Robb, J. R. Cheeseman, G. Scalmani, V. Barone, B. Mennucci,, G. A. Petersson, H. Nakatsuji, M. Caricato, X. Li, H. P. Hratchian, A. F. Izmaylov, J. Bloino, G. Zheng, J. L. Sonnenberg, M. Hada, M. Ehara, K. Toyota, R. Fukuda, J. Hasegawa, M. Ishida, T. Nakajima, Y. Honda, O. Kitao, H. Nakai, T. Vreven, J. A. Montgomery, Jr.J. E. Peralta, F. Ogliaro, M. Bearpark, J. J. Heyd, E. Brothers, K. N. Kudin, V. N. Staroverov, T. Keith, R. Kobayashi, J. Normand, K. Raghavachari, A. Rendell, J. C. Burant, S. S. Iyengar, J. Tomasi, M. Cossi, N. Rega, J. M. Millam, M. Klene, J. E. Knox, J. B. Cross, V. Bakken, C. Adamo, J. Jaramillo, R. Gomperts, R. E. Stratmann, O. Yazyev, A. J. Austin, R. Cammi, C. Pomelli, J. W. Ochterski, R. L. Martin, K. Morokuma, V. G. Zakrzewski, G. A. Voth, P. Salvador, J. J. Dannenberg, S. Dapprich, A. D. Daniels, O. Farkas, J. B. Foresman, J. V. Ortiz, J. Cioslowski, D. J. Fox, *Gaussian 09, Revison D.01* Wallingford, CT, USA: Gaussian, Inc. **2009**.

[56] M. Valiev, E. J. Bylaska, N. Govind, K. Kowalski, T. P. Straatsma, H. J. J. Van Dam, D. Wang, J. Nieplocha, E. Apra, T. L. Windus, et al., *Comput. Phys. Commun.* **2010**, *181*, 1477.

[57] D. Gleeson, G. Sankar, C. Richard A. Catlow, J. Meurig Thomas, G. Spanó, S. Bordiga, A. Zecchina, C. Lamberti, *Phys. Chem. Chem. Phys.* **2000**, *2*, 4812.

[58] G. Artioli, C. Lamberti, G. L. Marra, *Acta Crystallogr. Sect. B Struct. Sci.* **2000**, *56*, 2.

[59] C. Lamberti, S. Bordiga, A. Zecchina, A. Carati, N. N. Fitch, G. Artioli, G. Petrini, M. Salvalaggio, G. L. Marra, *J. Catal.* **1999**, *183*, 222.

[60] P. Glatzel, U. Bergmann, *Coord. Chem. Rev.* **2005**, *249*, 65.

[61] J. Singh, C. Lamberti, J. A. van Bokhoven, *Chem. Soc. Rev.* **2010**, *39*, 4754.

[62] E. Gallo, C. Lamberti, P. Glatzel, *Phys. Chem. Chem. Phys.* **2011**, *13*, 19409.

[63] C. Lamberti, S. Bordiga, A. Zecchina, G. Artioli, G. Marra, G. Spanò, *J. Am. Chem. Soc.* **2001**, *123*, 2204.